Int J Adv Struct Eng (2015) 7:69–80
DOI 10.1007/s40091-015-0084-7

ORIGINAL RESEARCH

Experimental and numerical evaluation of wavelet based damage detection methodologies

Mireya M. Quiñones · Luis A. Montejo · Shinae Jang

Received: 5 March 2014 / Accepted: 5 February 2015 / Published online: 13 February 2015

Abstract This article presents an evaluation of the capabilities of wavelet-based methodologies for damage identification in civil structures. Two different approaches were evaluated: (1) analysis of the structure frequencies evolution by means of the continuous wavelet transform and (2) analysis of the singularities generated in the high frequency response of the structure through the detail functions obtained via fast wavelet transform. The methodologies were evaluated using experimental and numerical simulated data. It was found that the selection of appropriate wavelet parameters is critical for a successful analysis of the signal. Wavelet parameters should be selected based on the expected frequency content of the signal and desired time and frequency resolutions. Identifications of frequency shifts via ridge extraction of the wavelet map were successful in most of the experimental and numerical scenarios investigated. Moreover, the frequency shift can be inferred most of the time but the exact time at which it occurs is not evident. However, this information can be retrieved from the spike location from the Fast Wavelet Transform analysis. Therefore, it is recommended to perform both type of analysis and look at the results together.

M. M. Quiñones
Department of Civil Engineering and Surveying, University of Puerto Rico at Mayaguez, Mayaguez, PR 00680, USA
e-mail: mireya.quinones@upr.edu

L. A. Montejo (✉)
Department of Engineering Science and Materials, University of Puerto Rico at Mayaguez, Mayaguez 00680, Puerto Rico
e-mail: luis.montejo@upr.edu

S. Jang
Department of Civil and Environmental Engineering, University of Connecticut, Storrs, CT 06269, USA
e-mail: sjang@engr.uconn.edu

Keywords Continuous wavelet transform · Discrete wavelet transform · Fast wavelet transform · Health monitoring · Damage detection

Introduction

Buildings, bridges, and other civil infrastructure can collapse during a natural or man-made damaging event. In the cases that the structure can withstand the wave propagation without collapse, there is a chance that the induced vibrations have caused an unknown level of damage. A structural assessment is then required to diagnose the health of the structure. While this information is the key for first responders to plan a safe and efficient post-disaster response, such task is challenging to accomplish as the response of a civil structure to a damaging event is a rather complex dynamic system with multiple elements and components that are in stressed interaction with one another.

This article explores the possibility of using the registered dynamic response from instrumented structures to identify the occurrence of damage. Moreover, the capabilities of wavelet transforms to extract information related to damage episodes imbedded in the acceleration response of the structure are evaluated. The methodologies evaluated are based on the premise that the occurrence of damage is reflected in changes in the instantaneous frequency of vibration of the structure and/or in discontinuities reflected in the high frequency response of the structure. While this type of approach has been previously explored, the validation and calibration have been performed mostly based on simulated data (e.g. Sone et al. 1995; Al-Khalidy et al. 1997; Hou and Noori 1999; Ovanesova and Suarez 2004; Hera and Hou 2004; Hou

et al. 2006; Montejo 2011; Montejo et al. 2012). The purpose of this research work is to validate and further calibrate wavelet-based detection algorithms using experimental data from two different test setups and simulated data from a multi-degree of freedom system. Special emphasis is placed on the influence of frequency content of the excitation, the presence of noise in the registered structural response and the system complexity on the efficiency of the methodologies. Finally, it should be mention that there are other types of wavelet based methodologies based on the sensibility of the wavelet coefficients (e.g. Walia et al. 2013; Reddy and Swarnamani 2013) which are out of the scope of this study.

Wavelet transforms for damage detection

Nowadays, the theory and numerical implementation behind wavelet transforms is widely available from books (e.g. Mallat 2009), technical articles (e.g. Montejo and Suarez 2013) and software documentation (e.g. Misiti et al. 2013). Therefore, in this manuscript only the most relevant aspects of wavelet transforms for its successful implementation in damage detection are addressed. Two type of wavelet analysis are performed: an analysis at low frequencies via the continuous wavelet transform to keep track of any frequency shifts in the structure and a high frequency analysis via the Fast Wavelet Transform to detect any singularities in the response of the structure.

Continuous wavelet transform (analysis of frequency shifts)

The continuous wavelet transform (CWT) of a signal $f(t)$ can be defined as the convolution the signal with scaled versions of a mother wavelet function Ψ as defined by Eq. 1.

$$C(s,p) = \int_{-\infty}^{+\infty} f(t)\Psi_{s,p}^{*}dt = \int_{-\infty}^{+\infty} f(t)\frac{1}{\sqrt{s}}\Psi^{*}\left(\frac{t-p}{s}\right)dt \tag{1}$$

The parameter s and p are used to scale and shift the wavelet, respectively. The asterisk * indicates complex conjugation and the normalizing factor $1/\sqrt{s}$ ensures that the energy is the same for all values of s. The result of the transform is a matrix of wavelet coefficients $C(s,p)$ that contain information about the signal at the scale s and time position p. That is, the CWT can be viewed as a two dimensional transform that maps an original time signal $f(t)$ into a time-scale domain. Since the scale s can be related to frequency, the CWT can be used to obtain simultaneous time–frequency representations of dynamic responses to track frequency shifts in the system natural frequencies (e.g. Aguirre et al. 2013).

The selection of the mother wavelet function plays a key role on the successful implementation of the analysis. For this application, the Modified Complex Morlet Wavelet (Yan et al. 2006, Eq. 2) was selected as it provides parameters that allow modification of the properties of the wavelet form according to the characteristics of the signal to be analyzed. Furthermore, this wavelet has been successfully used in the past for the analysis of vibrational signals (e.g. Montejo and Vidot 2012):

$$\psi(t) = \frac{1}{\sqrt{\pi f_b}} e^{i2\pi f_c t} e^{-t^2/f_b} \tag{2}$$

where f_b is a bandwidth parameter that controls the shape of the mother wavelet and f_c is the central frequency of the mother wavelet. Using the Heisenberg uncertainty principle it can be shown that the time and frequency resolutions for this wavelet at a frequency f_i are given by:

$$\Delta t_i = \frac{f_c}{f_i}\frac{\sqrt{f_b}}{2} \quad \text{and} \quad \Delta f_i = \frac{f_i}{f_c}\frac{1}{2\pi\sqrt{f_b}} \tag{3}$$

The toy signal displayed in Fig. 1 is used to demonstrate the application of the CWT and to calibrate the wavelet parameters to be used for the analysis of one of the sets of experimental data that will be later presented. The sampling frequency was 1,024 Hz and the duration of the signal was 40 s, the signal consists of two sinusoidal waves of 21 and 24 Hz, with a discontinuity at 20 s when the frequencies are shifted to 21.9 and 24.5 Hz, respectively. Figure 1 shows the signal in both, the time and frequency domains. The wavelet coefficients $W(s,p)$ resulting from applying the CWT are shown in its absolute values in the wavelet maps displayed in Fig. 2. In these maps the color patterns show the high value coefficients used to detect the dominant frequency. From the color intensity the ridges can be extracted, which are also used to determine the instant frequencies in the signal. The ridges can be extracted by a variety of techniques (e.g., Carmona et al. 1997). The instantaneous dominant frequencies in Fig. 2 were obtained by locating the local maxima at each time instant. The analysis was performed using different values for f_b and f_c to show the importance of these parameters to obtain a good resolution and identify the shift over time in the frequency content of the signal. Figure 2 (top) shows the results obtained using $f_b = 1$ and $f_c = 1$, it is seen that these parameters are not appropriate to identify the frequencies. This is in agreement with the corresponding frequency resolution obtained for these parameters from Eq. 3, $\Delta f = 3.8$ Hz ($fi = 24$ Hz) which is not enough to separate the two tones in the signal. On the other hand, good results are obtained using $f_b = 30$ and $f_c = 15$, with

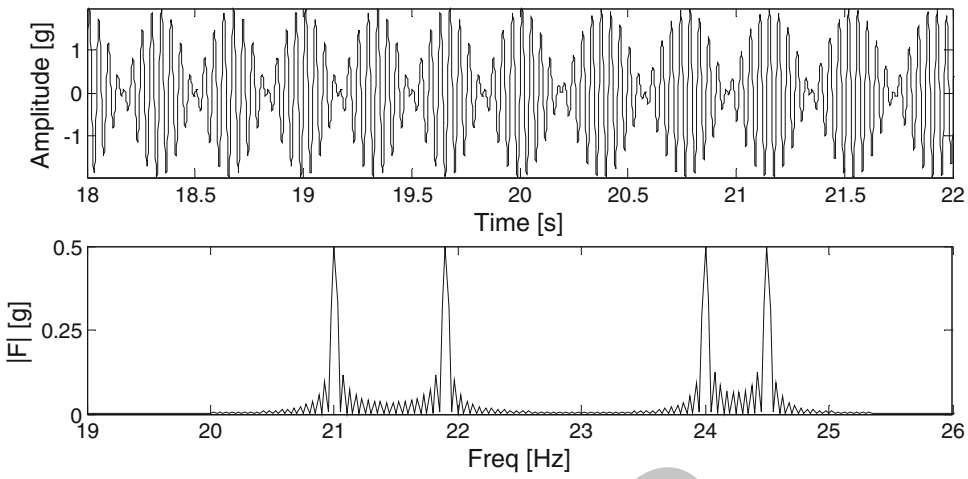

Fig. 1 Toy signal in the time (*top*, only 4 s shown in the sake of clarity) and frequency (*bottom*) domains

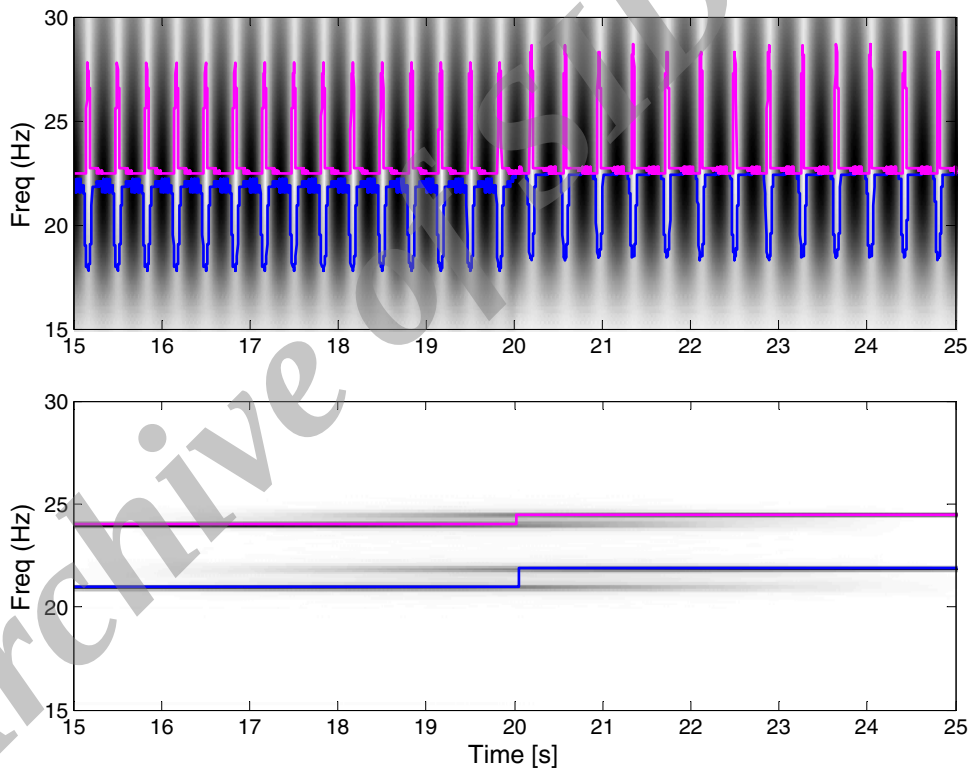

Fig. 2 CWT analysis using wavelet parameters $fc = 1$ $fb = 1$ (*top*) and $fc = 15$ $fb = 30$ (*bottom*)

critical resolution values of $\Delta t = 1.96$ s ($fi = 21$ Hz) and $\Delta f = 0.046$ *Hz* ($fi = 24$ Hz) as shown in Fig. 2 (bottom).

Fast wavelet transform (analysis of high frequency singularities)

In the discrete wavelet transform (DWT) the values of scale and position used to perform the analysis are chosen based on a dyadic scale (i.e. based on powers of 2, 2^j). For some special mother wavelets $\psi(t)$ the corresponding discretized wavelets $\psi_{s,p}(t)$ constitute an orthonormal basis. Mallat (1989) developed the fast wavelet transform (FWT), a fast wavelet decomposition and reconstruction algorithm for implementation of DWT that employs a two-channel sub-band coder. In the FWT a signal can be represented (Eq. 4) by its approximations (A) and details (D) at different levels of decomposition (j). The approximations are the high scale, low-frequency components of the signal. The details are the low-scale, high-frequency components.

$$f(t) = A_j + \sum_{i \le j} D_i \tag{4}$$

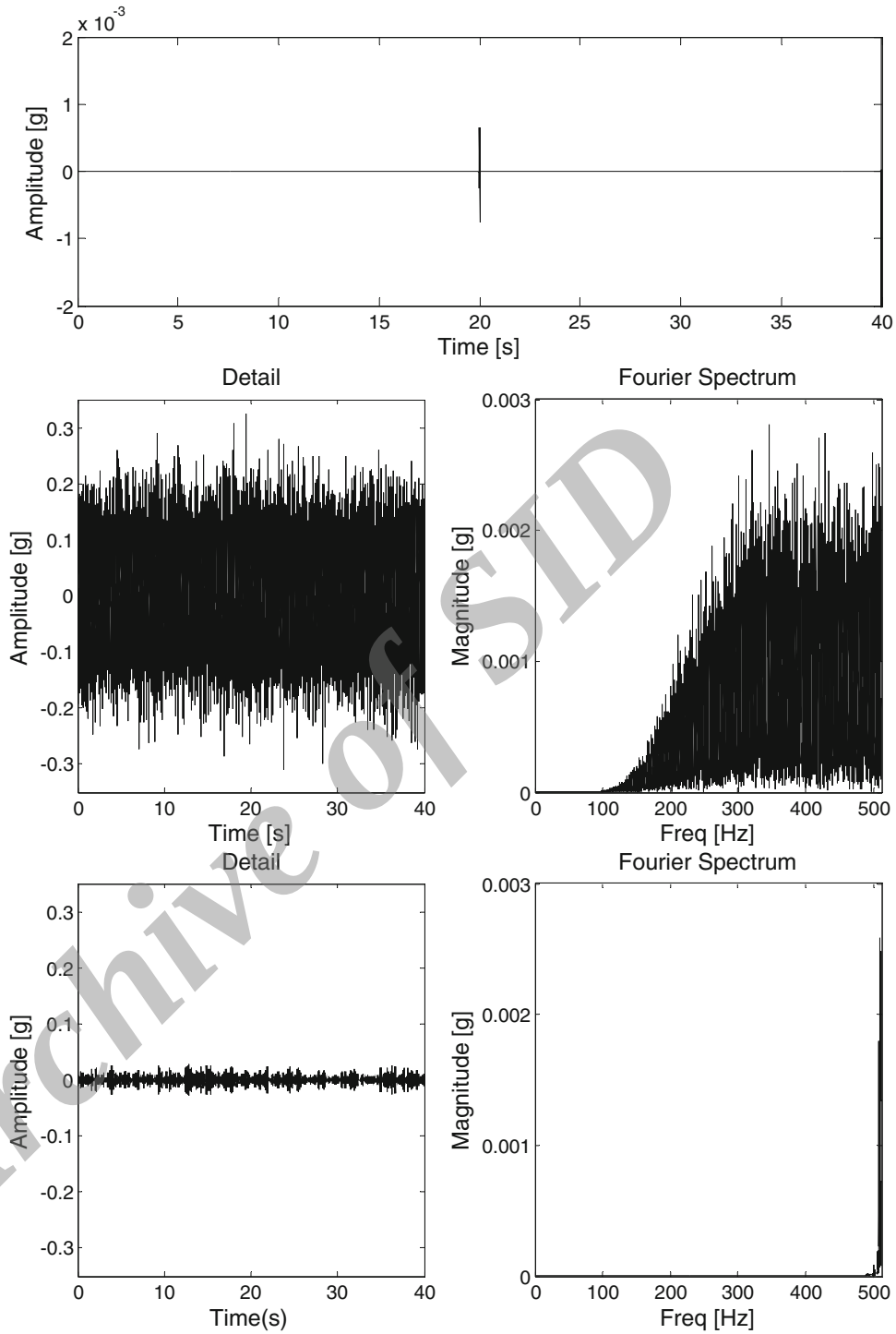

Fig. 3 Detail function for the first level of decomposition for the clean signal (*top*), detail function for the first level of decomposition for the signal with SNR = 100 along with its Fourier spectrum (*middle*) and detail function for the seventh level of decomposition for the signal with SNR = 100 along with its Fourier spectrum (*bottom*)

Damage detection using the FWT is relatively simple; in this work we used the FWT implementation available in the Matlab to decompose the signal in its approximation and detail functions. Once the detail function is obtained we look for spikes on it, if no spikes are present one can refine the analysis by performing the next decomposition level (i.e. decomposing the first level detail function into additional approximation and detail functions, and so on). For example, using the toy signal generated before (Fig. 1) we can apply the FWT analysis to detect the discontinuity embedded in the signal. Figure 3 (top) shows the detail functions obtained at the first level of decomposition using the Bior6.8 wavelet (notice that the Complex Morlet Wavelet used for the CWT cannot be used to implement

the FWT). It seen that a spike appears in the detail function that can be clearly related to the discontinuity caused in the signal. As this methodology is based on the analysis of the high frequency content of the signal, it can be very sensible to noise contamination. To examine this issue, Gaussian noise with a SNR of 100 (i.e. very low noise) was added to the signal. The result obtained at the first level of decomposition (i.e. frequency content between 256 and 512 Hz, as reflected in its Fourier spectrum) is shown in Fig. 3 (middle), it is seen that this time the discontinuity got embedded in the added noise. Additional decompositions were performed to check if the discontinuity could be detected from a different detail function with narrower frequency content but the results were no successful, Fig. 3 (bottom) shows for example the results for the level 7 of decomposition (detail function with frequency content between 504 and 508 Hz).

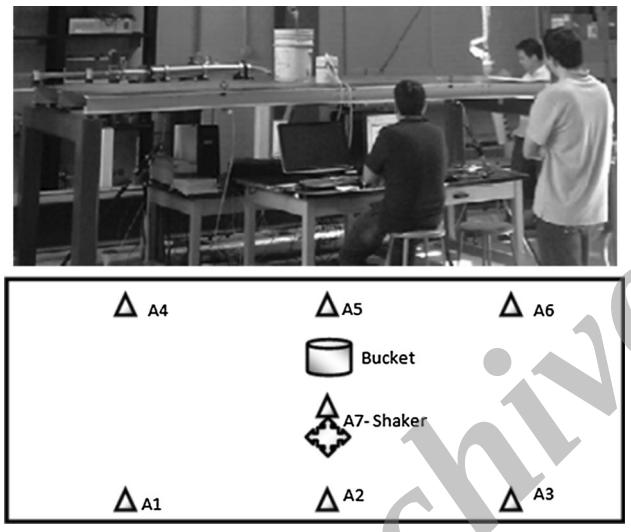

Fig. 4 Test setup and distribution of the accelerometers (*top view*)

Implementation and results

The two approaches previously described were evaluated under more realistic scenarios using data from two experimental setups (a single span bridge model and a twelve bay steel truss bridge model) and a numerical simulation of a shear building under seismic excitation.

Single span bridge

A single span steel bridge was used to simulate a damage scenario by adding and removing mass through a 20.2 kg bucket connected to the laboratory crane while the bridge was subjected to low amplitude noise excitation (Fig. 4). The structure was excited with different vertical white noise vibrations using a shaker located near the middle of the span and the acceleration response was measured by 7 piezoelectric accelerometers (Fig. 4). Accelerometer number 7 measured the vibrations imposed by the shaker. A preliminary identification of the structure natural frequencies of vibration was accomplished using a free decay test. Then, the response of the structure to white noise excitations of different frequency content (0–100 Hz, 0–80 Hz, 0–60 Hz, 0–40 Hz and 0–30 Hz) was analyzed. The objective was to identify real-time dynamic changes caused by the added and removed mass on each test. The frequencies estimated from the free decay are used as target values and to generate the toy signal (previously described) for wavelet parameter calibration.

The total excitation duration was 40 s. At around 20 s, 20.2 kg are added or removed from the bridge to induce a change in the dynamic properties. The sampling frequency for all tests is 1,024 Hz. Figure 5 show the recorded accelerations in the middle of the span, it is seen that for the added mass cases the instant when the discontinuity occurs

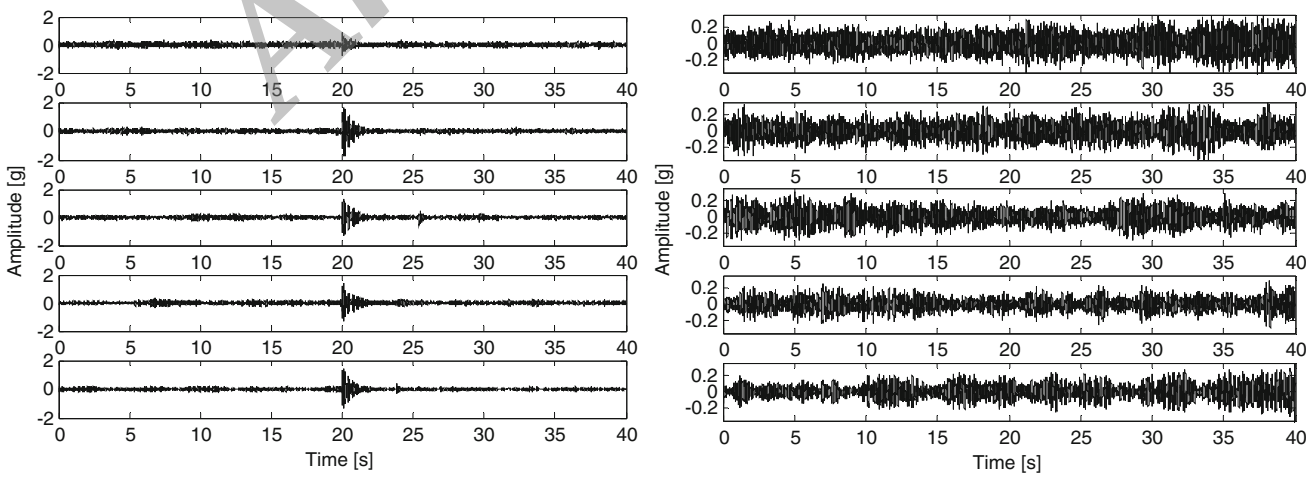

Fig. 5 Recorded accelerations at mid-span of the bridge, 0–100 Hz to 0–30 Hz (*top* to *bottom*). *Left* added mass cases, *right* removed mass cases

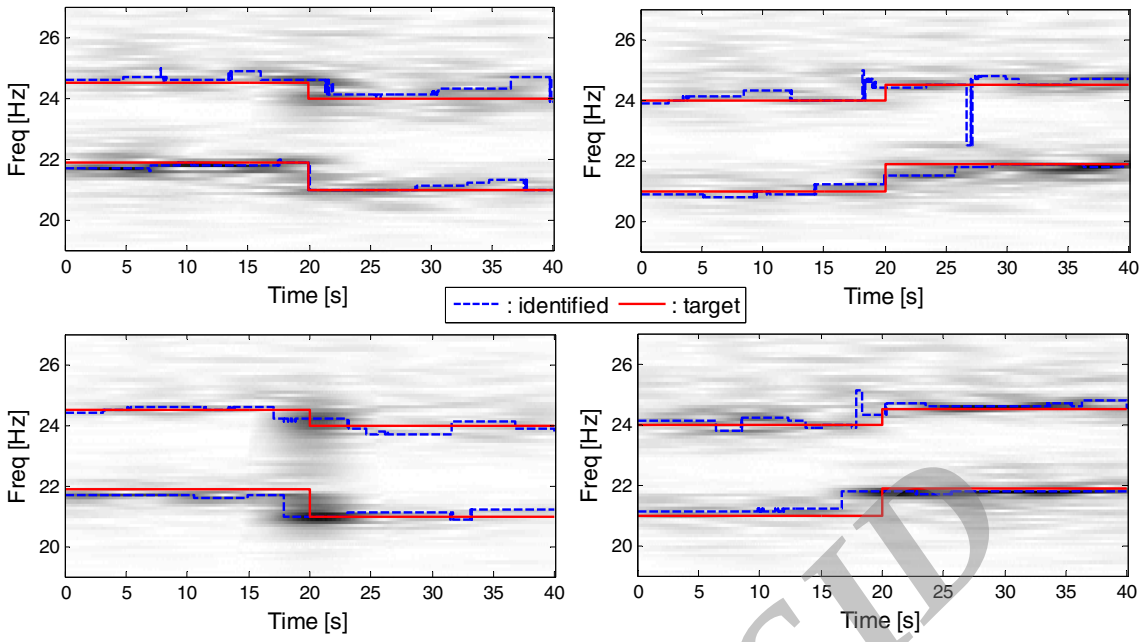

Fig. 6 Low frequency CWT analysis of the accelerations measured in the middle of the span with a noise excitation frequency content in the ranges 0–100 Hz (*top*) and 0–30 Hz (*bottom*). *Left* mass added, *right* mass removed

due to the mass added is evident as a spike with an amplitude about 10 times current acceleration levels is produced. However, for the removed mass cases it is not possible to detect the discontinuity at simply view.

In the various tests performed, the results obtained revealed similar patterns. Figure 6 (top) shows the results when the frequency content of the white noise excitation is in the range 0–100 Hz and the mass is added or removed during the test. The same results are shown in Fig. 6 (bottom), but for a noise excitation with frequency content in the range 0–30 Hz. The data analyzed consists of the accelerations acquired at the mid-span (sensor #2). In the wavelet maps the darker shades represent the occurrence of higher valued CWT coefficients. The extracted ridges are represented by the dashed lines (time domain frequencies) and the solid lines depict the target frequencies. It is seen that the identification of the shifts in frequency does not depend on the frequency content of the excitation. From Eq. 3, for the 21 Hz tone the frequency resolution is 0.041 Hz while for the 24 Hz tone the resolution is 0.046 Hz. That is, the frequency resolution of the analysis is enough to identify and separate both modes. The various white noise excitations resulted in a similar wavelet map.

FWT analyses were performed attempting to point out the exact instant when the discontinuity occurs. The results obtained using the acceleration recorded in the middle of the span (sensor #2) show similar behavior for the all cases analyzed. Figure 7 shows the results when the frequency content of the noise excitation is 0–100 Hz and 0–30 Hz. The discontinuity can be detected in all cases using FWT at first level of decomposition, it is also seen that when the mass is added the magnitude of the spike is larger compared with the removed mass case. It should be noticed that from the toy signal used for calibration it was not possible to determine via FWT the spike of the discontinuity when a minimum level of noise was added (Fig. 3). This can be explained by the way the mass was added and removed from the bridge: when the bucket is lifted or sited in the bridge an additional disturbance is added into the system response which was not modeled in the toy signal, that additional disturbance is likely to be the anomaly detected in the experimental data. Figure 8 shows the maximum absolute value of the magnitudes of the DWT analyses. It is seen that the location of the maximum values changes from case to case, therefore the spike relative amplitudes cannot be used to determine the location of the disruption.

Twelve bay steel truss bridge

A simple-supported 12 bay steel bridge (Fig. 9) was used to simulate a damage scenario by the removal of mass while the structure is being excited by low amplitude white noise. Three different mass set-ups were considered: (1) a single mass concentrated in the middle, (2) four masses at ¼ of the span and (3) four masses around the middle of the span. The bridge is supported by a roller support on one side and a pin support on the other side. The bridge is made of 1,045 steel with 0.07 in diameter circular section members and length 15.5 in for the vertical members, 23.8

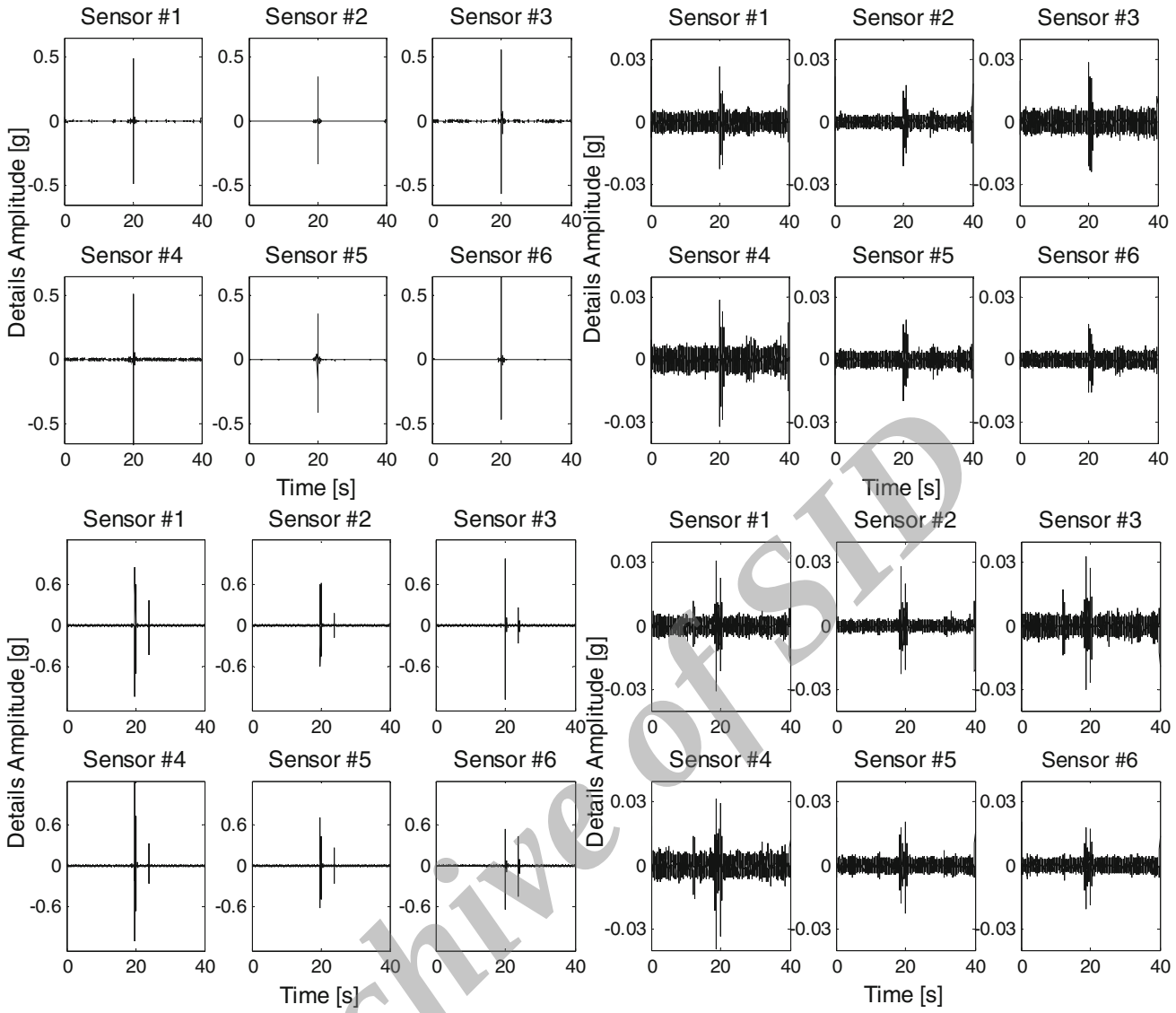

Fig. 7 High frequency analysis at first level of decomposition via FWT for all sensors along the span with a noise excitation frequency range of 0–100 Hz (*top*) and 0–30 Hz (*bottom*). *Left* mass added, *right* mass removed

in for the diagonal members and 18 in for the horizontal members resulting in an overall bridge length of 216 inches from the truss arrangement. The structure was excited using a shaker located in the middle of the span and the acceleration response was measured by 11 piezoelectric accelerometers at the bottom joints of the bridge (Fig. 9), sensor 12 is measuring the shaker excitation.

A preliminary identification of the natural frequencies was performed using the free decay response of the structure (impact hammer test) with different added masses. These frequencies are used as targets to analyze the response of the structure to white noise excitations of different frequency content (0–200 Hz, 0–150 Hz, 0–100 Hz and 0–50 Hz). As for the previous setup, the objective is to identify real-time dynamic changes provoked by the removal of different amounts of masses ranging from 12 to 3 kg on each test.

In this set of tests, the bridge is excited by white noises with different frequency contents while the accelerometers record the structural response. In the sake of brevity only the results obtained for the third case as this constitutes the most general and challenging set up. In this case four masses adding a total of 12 kg mass were located around the middle of the span and every 50 s 3 kg are removed. Following the same approach described for the single span bridge, a toy signal was generated to obtain optimal parameters for the Complex Morlet Wavelet. The values obtained were $f_b = 30$ and $f_c = 4$, the critical resolution values are then $\Delta t = 0.58$ s ($f_i = 19$ Hz) and $\Delta f = 0.26$ Hz ($f_i = 36$ Hz). Figure 10 shows the results

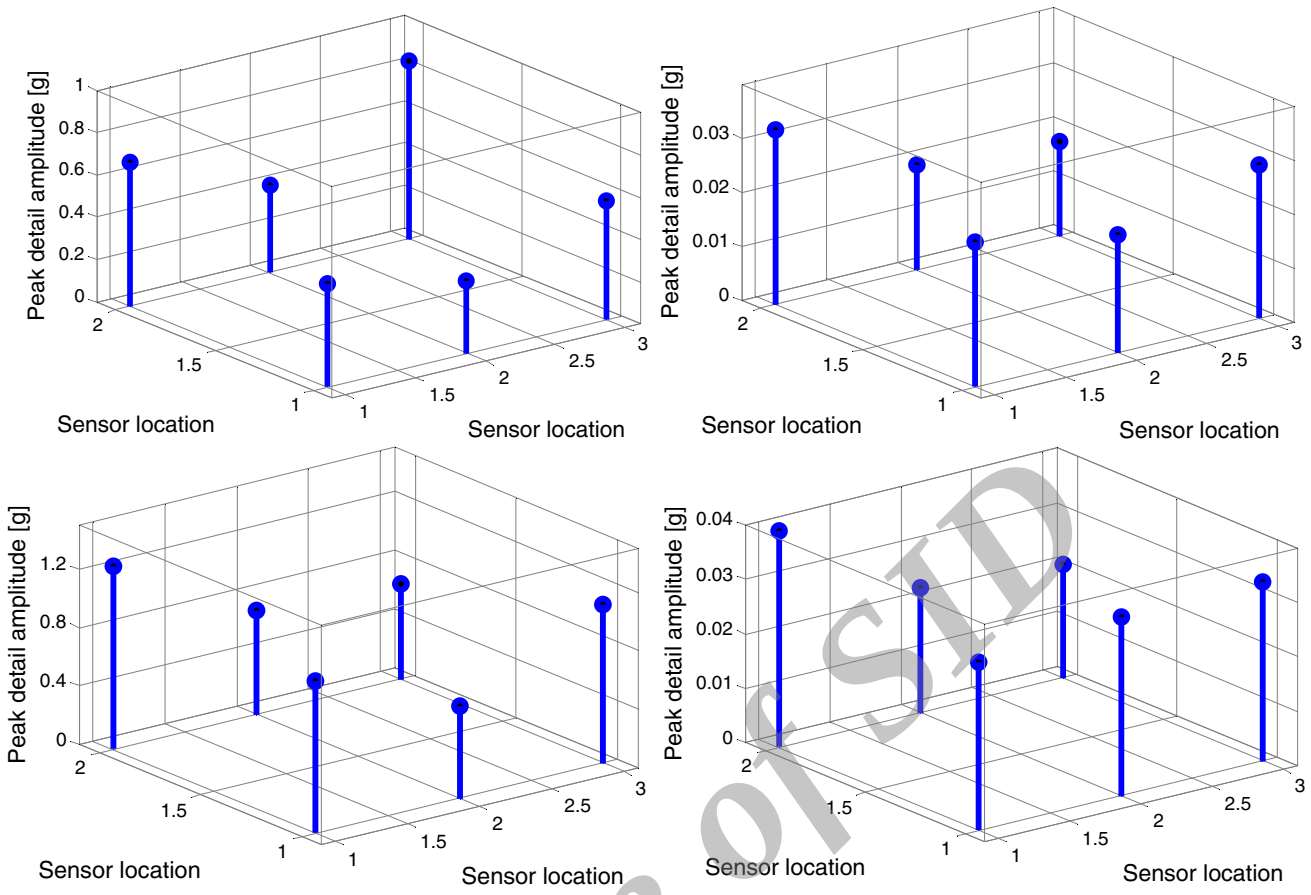

Fig. 8 Maximum absolute value results of DWT for all sensors along the span with a noise excitation frequency range of 0–100 Hz (*top*) and 0–30 Hz (*bottom*). *Left* mass added, *right* mass removed

Fig. 9 Steel truss bridge and sensor distribution

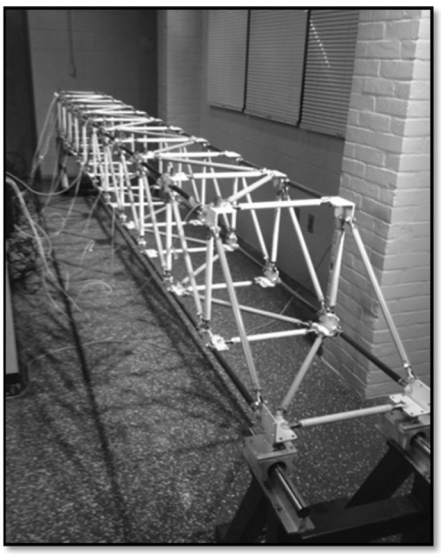

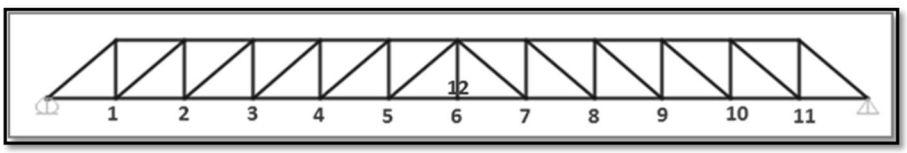

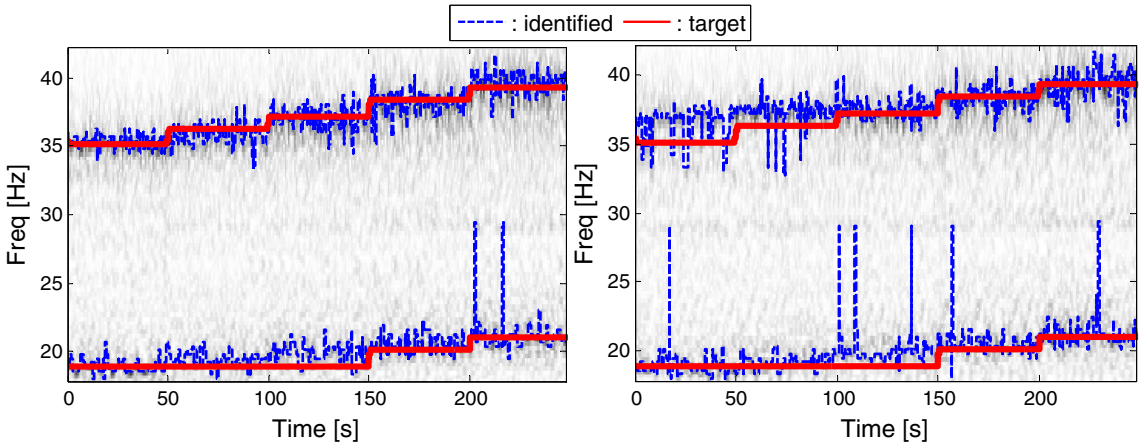

Fig. 10 CWT analysis for case 3. *Left* noise excitation frequency content of 0–200 Hz, *right* noise excitation frequency content of 0–50 Hz

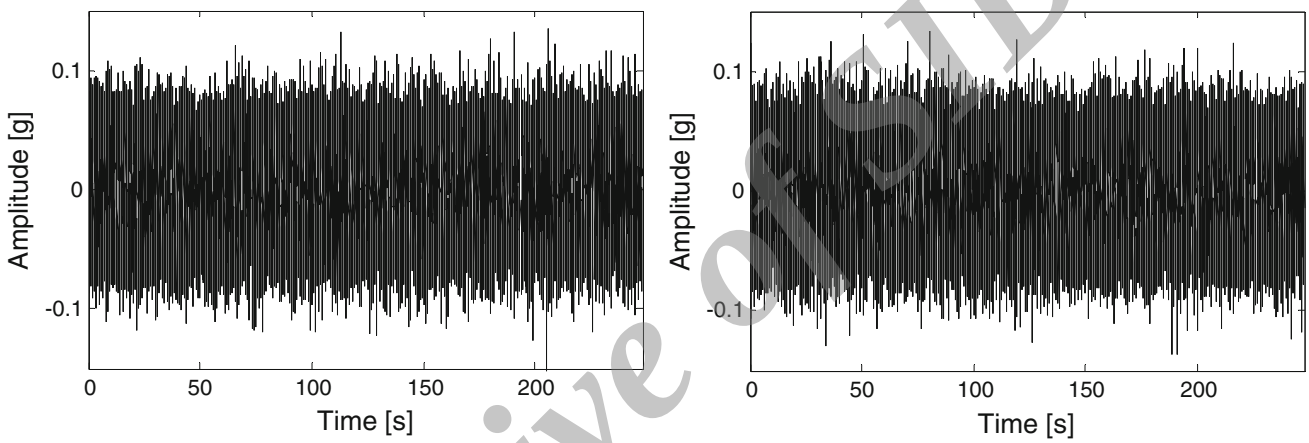

Fig. 11 High frequency analysis at first level of decomposition via FWT. *Left* noise excitation frequency content of 0–200 Hz, *right* noise excitation frequency content of 0–50 Hz

obtained for the two extreme noise excitation cases, the two first modes of the structure are identified and, as expected, there is an increase in the natural frequency values as the different masses are removed. Moreover, it is seen that the shifts in the frequencies are identified as they occur in time and the results of the analysis is not influenced by the frequency content of the excitation.

Fast Wavelet Transform analyses were performed to detect the instant when the discontinuities occur. The results obtained using the acceleration recorded in the middle of the span (sensor #6) show similar behavior for the three mass arrangements analyzed, Fig. 11 shows the results for the third case at the first level of decomposition, it is seen that the discontinuity is not significant enough to be detected. The results did not improve by increasing the level of decomposition. Most likely, this is due to the low disturbance caused in the system when the masses were removed, when compared for example, to the procedure used in the single span bridge. This causes the singularities in the response to get imbedded in the signal noise and make them difficult to detect.

Shear building numerical model

A numerical model of a five story shear building was developed and subjected to seismic accelerations at the base while the stiffness of the first floor is suddenly reduced (from one time step to the next) to simulate the effect of an abrupt damage localized at this level (Fig. 12). The three main objectives with this numerical test are to: (1) determine the minimum level of damage that can be detected by wavelet-based methodologies in this type of structures; (2) investigate the effect of noise contamination on the efficiency of the methodologies being evaluated and (3) verify if the amplitude of the spikes detected in the FWT detail functions can be related to the level and localization of the damage. To accomplish these objectives, a number of

numerical tests were performed with different stiffness reduction factors and noise levels.

The mass and stiffness at each floor were specified as 4,000 kg and 5 × 10^6 N-m, respectively. The damping ratio was set at 5 % for all modes. The seismic input used corresponds to a record from the 1,980 M7 Trinidad (California) earthquake, and the sampling frequency was 200 Hz. The responses of the structure to the earthquake excitation using different damage levels (90, 50, 30, 20, 10 and 5 % reduction in the first floor stiffness) were generated. In addition, different levels of noise (SNR = 100, 20, 5, 1) were added to each case. The natural frequencies before and after damage calculated by solving the eigenvalue problem were used as target frequency values in the CWT analyses, the natural frequencies of the pristine building ranged from 1.6 to 10.8 Hz. Using a toy signal for calibration purposes, values of $f_b = 6$ and $f_c = 2$ were found appropriate to define the mother Complex Morlet Wavelet.

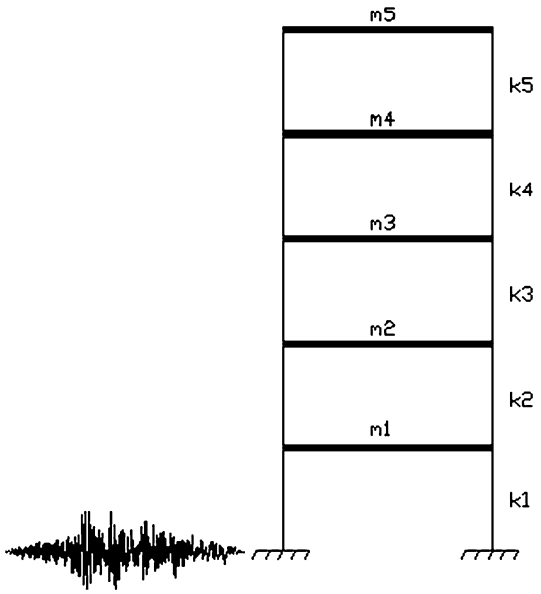

Fig. 12 Five-story shear building excited by the 1980 M7 Trinidad (California) earthquake

Figure 13 shows the results for the accelerations in the first floor at 30 % damage with SNR = 100. The left figure shows the Fourier spectrum where it is seen that the peaks coincide with the modal frequencies of the structure. In the wavelet map (right figure) the darker shades represent the occurrence of higher valued CWT coefficients. The extracted ridges are represented by the dashed lines and the solid lines depict the target frequencies. It is seen in the CWT results that it was possible determine the frequency shift for a few modes of the structure. It is more difficult detect the frequency shift at the upper modes. This is due to a combination of two phenomena: (1) the expected frequency shift in the upper modes is less significant than for the first modes and the frequency resolution deteriorates as the frequency increases (e.g. for 1.6 Hz the frequency resolution is 0.05 Hz while for 4.7 is 0.15 Hz). Similar results were obtained for all the other cases of different

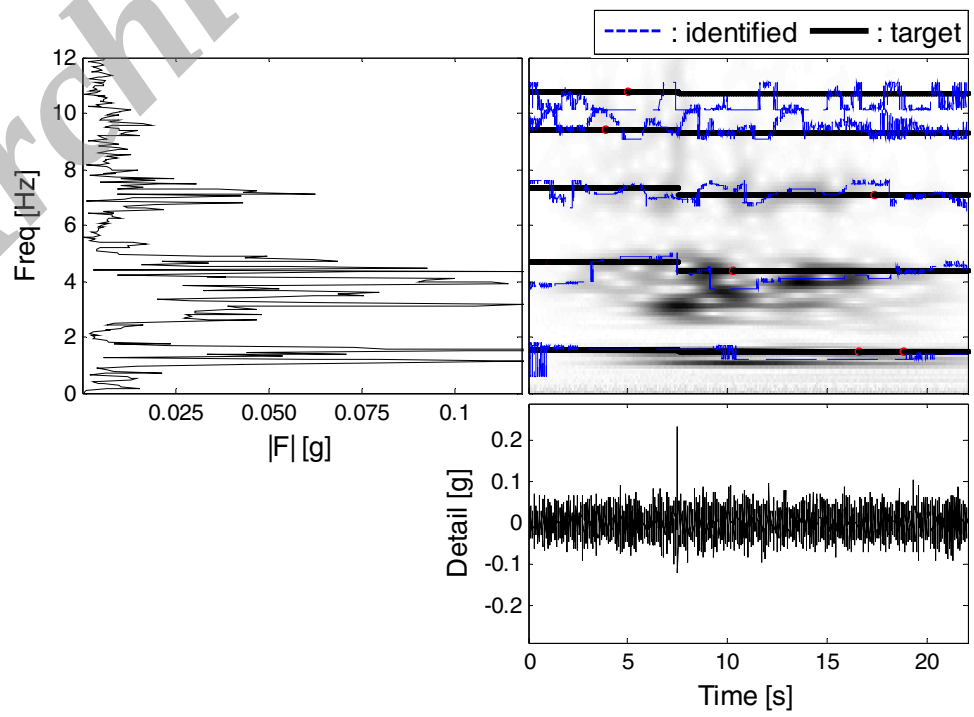

Fig. 13 Results obtained at the first floor, 30 % damage with SNR = 100. *Left* fourier spectrum. *Right* low frequency CWT analysis (*top*); high frequency FWT analysis (*bottom*)

damage level, as expected the extracted ridges start to deteriorate as the level of damage decreases and the noise contamination increases.

In the FWT results (Fig. 13, bottom figure) it can be observed that a large spike emerge at the time instant where the sudden stiffness reduction was induced. As for the CWT analyses, the results deteriorate as noise increases and damage decreases. The discontinuity was detected from all floors only when the signals were clean. Once noise was incorporated to the signals, the discontinuity is only detectable from the accelerations at the first floor and stiffness reductions larger than 20 %; Table 1 summarizes the results obtained. For the cases where the identification was possible at all floor levels (i.e. the cases without noise contamination), the amplitude of the spikes was related to the proximity to the location of the damage, that is, the largest spike amplitude occurred at the first floor and the smallest at the top floor (Fig. 14). Moreover, a correlation was also found between the level of damage and the amplitude of the spike (Fig. 15).

Table 1 Effect of noise contamination and induced damage level on FWT-based damage detection results

	Noise level (SNR)				
	∞	100	20	5	1
Stiffness reduction					
90 %	5	1	1	1	0
50 %	5	1	1	0	0
30 %	5	1	0	0	0
20 %	5	0	0	0	0
10 %	5	0	0	0	0
5 %	5	0	0	0	0

A 5 indicates that the damage was detected from the response of the 5 floors, a 1 indicates that the damage was only detected from the response measured at the first floor, a 0 indicates that the damage was no detected

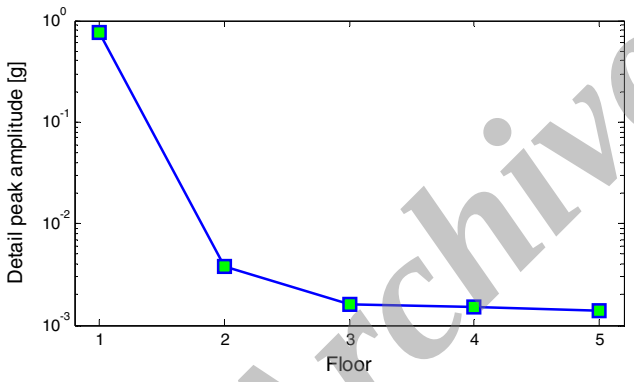

Fig. 14 Maximum amplitude of the details spike at each floor for the case without noise

Conclusions

Two different wavelet-based damage detection approaches were evaluated using experimental and simulated data. One of the approaches is based on the tracking of frequency shifts using the continuous wavelet transform (CWT) while the second approach is aimed to identify singularities in the high frequency component of the structural response via the Fast Wavelet Transform (FWT). Based on the results obtained the following conclusions/recommendations are drawn:

Continuous wavelet transform

It was found that selection of appropriate wavelet parameters is critical for a successful analysis of the signal via CWT. Wavelet parameters should be selected based on the expected frequency content of the signal and desired time and frequency resolutions. When clean toy signals and appropriate wavelet parameters are used, the performance of the CWT for frequency tracking is ideal. Identification of frequency shifts via ridge extraction of the Wavelet Map was successful in most of the experimental and numerical

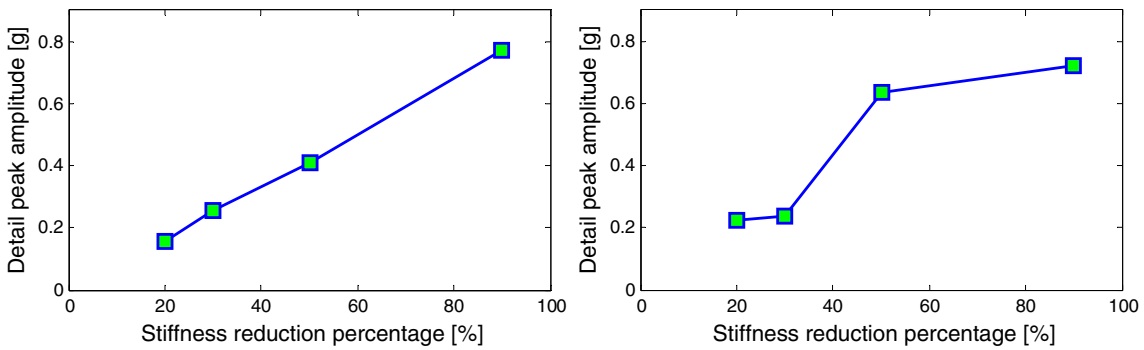

Fig. 15 First floor peak detail amplitude at different stiffness reduction percentages. *Left* SNR = 100, *right* SNR = 20

scenarios investigated. Moreover, the frequency shift can be inferred most of the time but the exact time at which it occurs is not that evident.

Fast wavelet transform

Fast Wavelet Transform analysis of the high frequency response of the structure to detect singularities induced by damage episodes was shown to be successful only at low levels of noise scenarios. Moreover, if the noise amplitude is larger than the discontinuity caused by the damage, the spike related to the damage episode will get imbedded within the noise in the signal. In the numerical model the amplitude of the FWT spikes was found to be related to the level of damage and the proximity of the sensor to the location were the damage was induced. Such correlation was not found on the experimental test, however, notice that this may be due the reduced scale nature of the setups employed. Other studies using large scale shake table test data of reinforced concrete columns have found that the discontinuity produced when a reinforcing bar fails during an earthquake is large enough to be detected via FWT (Aguirre et al. 2013).

It must be noticed that for testing convenience, in the two experimental setups analyzed in this work the damage scenario (mass added/removed) differs from what is usually expected in an actual structure (stiffness degradation). However, the resulting effects in the dynamic response of the structure are of the same nature, i.e. a shift in the natural frequencies of vibration. Moreover, all of the cases analyzed (experimental and numerical) a sudden damage scenario is recreated (typical for example of a shear failure), in the case were damage evolves slowly a discontinuity at high frequencies is not likely to occur, but the natural frequencies shift can still be tracked.

Acknowledgments This research was performed under an appointment to the U.S. Department of Homeland Security (DHS) Summer Research Team Program for Minority Serving Institutions, administered by the Oak Ridge Institute for Science and Education (ORISE) through an interagency agreement between the U.S. Department of Energy (DOE) and DHS. ORISE is managed by Oak Ridge Associated Universities (ORAU) under DOE contract number DE-AC05-06OR23100. All opinions expressed in this paper are the author's and do not necessarily reflect the policies and views of DHS, DOE or ORAU/ORISE. Additional support was received from the Puerto Rico Strong Motion Program at the Civil Engineering Department of the University of Puerto Rico at Mayaguez. The experimental tests were performed at the Smart Infrastructure Laboratory at the Department of Civil and Environmental Engineering at the University of Connecticut.

References

Aguirre DA, Gaviria CA, Montejo LA (2013) Wavelet-based damage detection in reinforced concrete structures subjected to seismic excitations. J Earthquake Eng 17(8):1103–1125

Al-Khalidy A, Noori M, Hou Z, Yamamoto S, Masuda A, Sone A (1997) Health monitoring systems of linear structures using wavelet analysis. In: Proceeding of the 1st International Workshop on Structural Health Monitoring, Stanford, CA

Carmona RA, Hwang WL, Torresani B (1997) Characterization of signals by the ridges of their Wavelet transforms. IEEE T. Signal Proc. 54(10):2586–2590

Hera A, Hou Z (2004) Application of wavelet approach for ASCE structural health monitoring benchmark studies. ASCE J Eng Mech 130(1):96–104

Hou Z, Noori M (1999) Application of wavelet analysis for structural health monitoring. In: Proceedings of the 2nd International Workshop on Structural Health Monitoring, Stanford, CA

Hou Z, Hera A, Shinde A (2006) Wavelet–based structural health monitoring of earthquake excited structures. Comput Aid Civil Infrastruct Eng 21:268–279

Mallat SG (1989) Theory for multiresolution signal decomposition: the wavelet representation. IEEE Trans Pattern Anal Mach Intell 11(7):674–693

Mallat S (2009) A Wavelet Tour of Signal Processing: The Sparse Way. Elsevier, Burlington

Misiti M, Misiti Y, Oppenheim G, Poggi JM (2013) Wavelet Toolbox: Starting Guide. The Mathworks, Natick

Montejo LA (2011) Signal processing based damage detection in structures subjected to random excitations. Struct Eng Mech 4(6):745–763

Montejo LA (2013) Suarez LE (2013) An improved CWT-based algorithm for the generation of spectrum-compatible records. Int J Adv Struct Eng 5:26

Montejo LA, Vidot AL (2012) Synchrosqueezed wavelet transform for frequency and damping identification from noisy signals. Smart Struct Syst 9(5):441

Montejo LA, Velazquez LR, Ramirez RI, Jang S (2012) Wavelet and HHT based identification of different levels of inelastic action in RC structures. In: 15th World Conference on Earthquake Engineering, Lisbon, Portugal

Ovanesova AV, Suarez LE (2004) Applications of wavelet transforms to damage detection of frame structures. Eng Struct 26:39–49

Reddy MD (2013) Swarnamani S (2013) Structural damage identification using signal processing method. Int J Adv Struct Eng 5:6

Sone A, Yamamoto S, Nakaoka A, Masuda A (1995) Health monitoring system of structures based on orthonormal wavelet transform. In: Proceedings of the ASME Pressure Vessels and Piping Conference, pp 161–167

Walia SK, Patel RK, Vinayak HK (2013) Parti R (2013) Joint discrepancy evaluation of an existing steel bridge using time-frequency and wavelet-based approach. Int J Adv Struct Eng 5:25

Yan BF, Miyamoto A, Bruhlier E (2006) Wavelet transform-based model parameter identification considering uncertainty. J Sound Vib 291:285–301